Stem Cell Reports
Article

OPEN ACCESS

Disruption of OCT4 Ubiquitination Increases OCT4 Protein Stability and ASH2L-B-Mediated H3K4 Methylation Promoting Pluripotency Acquisition

Shuang Li,[1,6] Feng Xiao,[2,6] Junmei Zhang,[3,4] Xiaozhi Sun,[1] Han Wang,[2] Yanwu Zeng,[1] Jing Hu,[1] Fan Tang,[1] Junjie Gu,[1] Yingming Zhao,[3,5] Ying Jin,[1,2,*] and Bing Liao[1,*]

[1]Basic Clinical Research Center, Renji Hospital, Department of Histology, Genetics and Developmental Biology, Shanghai Key Laboratory of Reproductive Medicine, Shanghai JiaoTong University School of Medicine, 227 South Chongqing Road, Shanghai 200025, China
[2]CAS Key Laboratory of Tissue Microenvironment and Tumor, Shanghai Institute of Nutrition and Health, CAS Center for Excellence in Molecular Cell Science, Shanghai Institutes for Biological Sciences, University of Chinese Academy of Sciences, Chinese Academy of Sciences, 320 Yueyang Road, Shanghai 200032, China
[3]Department of Biochemistry, University of Texas Southwestern Medical Center, Dallas, TX 75390, USA
[4]Present address: Department of Pharmaceutical Sciences, School of Pharmacy, University of Pittsburgh, PA 15261, USA
[5]Present address: Ben May Department for Cancer Research, University of Chicago, Chicago, IL 60637, USA
[6]Co-first author
*Correspondence: yjin@sibs.ac.cn (Y.J.), liaobing@shsmu.edu.cn (B.L.)
https://doi.org/10.1016/j.stemcr.2018.09.001

SUMMARY

The protein level of OCT4, a core pluripotency transcription factor, is vital for embryonic stem cell (ESC) maintenance, differentiation, and somatic cell reprogramming. However, how OCT4 protein levels are controlled during reprogramming remains largely unknown. Here, we identify ubiquitin conjugation sites of OCT4 and report that disruption of WWP2-catalyzed OCT4 ubiquitination or ablation of *Wwp2* significantly promotes the efficiency of pluripotency induction from mouse embryonic fibroblasts. Mechanistically, disruption of WWP2-mediated OCT4 ubiquitination elevates OCT4 protein stability and H3K4 methylation level during the reprogramming process. Furthermore, we reveal that OCT4 directly activates expression of *Ash2l-b*, and that ASH2L-B is a major isoform of ASH2L highly expressed in ESCs and required for somatic cell reprogramming. Together, this study emphasizes the importance of ubiquitination manipulation of the reprogramming factor and its interplay with the epigenetic regulator for successful reprogramming, opening a new avenue to improve the efficiency of pluripotency induction.

INTRODUCTION

Pluripotent stem cells (PSCs), including embryonic stem cells (ESCs) and induced PSCs (iPSCs), possess the properties of unlimited self-renewal and pluripotent differentiation potential, enabling them valuable for both basic research and regenerative medicine. ESCs are established from the inner cell mass of the mammalian preimplantation blastocyst (Evans and Kaufman, 1981; Thomson et al., 1998), whereas iPSCs are derived from somatic cells by enforced expression of reprogramming factors, such as OCT4, SOX2, KLF4, and c-MYC (OSKM) (Takahashi et al., 2007; Takahashi and Yamanaka, 2006). To fulfill their potential, it is necessary to elucidate the regulatory mechanisms underlying the self-renewal and pluripotency of PSCs. Transcription factors, epigenetic regulators, and signaling pathways have been known to determine PSC fate coordinately. However, the precise mechanism by which transcription factors and epigenetic regulators interplay to establish and maintain pluripotency awaits further investigation.

Octamer-binding transcription factor 4 (OCT4), a homeodomain-containing transcription factor of the Pit-Oct-Unc (POU) family, is one of the most important transcription factors involved in ESC maintenance and pluripotency induction from somatic cells (Kim et al., 2009a, 2009b; Nichols et al., 1998). Interestingly, levels of OCT4 expression could determinate the cell fate of PSCs *in vitro* (Niwa et al., 2000). Mounting evidence shows that, in addition to transcriptional regulation, post-translational modifications, including ubiquitination (Liao and Jin, 2010; Xu et al., 2004, 2009), sumoylation (Wei et al., 2007; Zhang et al., 2007), O-GlcNAcylation (Jang et al., 2012), and phosphorylation (Liu et al., 2017; Saxe et al., 2009), play critical roles in controlling OCT4 expression levels and the fate of PSCs as well. We previously reported that WWP2, a member of the HECT ubiquitin (Ub) ligase family, is a specific E3 Ub ligase of OCT4 promoting its ubiquitination/degradation and inhibiting OCT4 transcriptional activity (Xu et al., 2004). Moreover, OCT4 could be sumoylated at lysine 118. In contrast to Ub modification, sumoylation of OCT4 enhances its protein stability, DNA binding ability, and transcriptional activity (Wei et al., 2007; Zhang et al., 2007). In addition, we found that WWP2 expedites OCT4 protein degradation during PSC differentiation. However, WWP2 has little impact on levels of OCT4 and its ubiquitination in undifferentiated mouse ESCs, indicating that WWP2 specifically controls OCT4 ubiquitination and protein stability during ESC differentiation (Liao and Jin, 2010). Our additional study found that ITCH, an E3 Ub ligase of the same HECT family as WWP2, could catalyze

OCT4 ubiquitination and elevate OCT4 transcriptional activity in undifferentiated mouse ESCs. Functionally, ITCH contributes to sustaining ESC characteristics and regaining pluripotency features from somatic cells (Liao et al., 2013). In line with our findings, Buckley et al. (2012) reported a systematic analysis of ubiquitination in pluripotency and cellular reprogramming, highlighting the ubiquitin-proteasome system as a key regulator of stem cell pluripotency, and the roles of Ub modification on some key pluripotency regulators, such as OCT4, NANOG, and c-MYC. However, it remains unexplored whether OCT4 ubiquitination is involved in the establishment of iPSCs.

In addition to transcription factors, epigenetic regulators are actively involved in pluripotency induction. In mammals, the highly conserved mixed lineage leukemia (MLL) family histone methyltransferases are responsible for catalyzing histone H3K4 methylation, generating genome-wide H3K4me1, -me2, and -me3 marks (Dou and Hess, 2008; Ruthenburg et al., 2007). The methyltransferase activity of MLL^{SET} relies on the core components of complexes, including WDR5, RbBP5, and ASH2L (Dou et al., 2006; Steward et al., 2006). Although H3K4 methylation, as well as WDR5, RbBP5, and DPY30, have been shown to be required for efficient iPSC derivation, how they contribute to cellular reprogramming is not completely understood. Particularly, the function of ASH2L in the pluripotency induction remains unclear. In addition, ASH2L has two prominent isoforms, ASH2L-A and ASH2L-B. Their contribution to pluripotency regulation has not been documented yet.

Here, we systematically investigate the function of WWP2-mediated OCT4 ubiquitination in reprogramming of mouse embryonic fibroblasts (MEFs), revealing that it represents a hurdle to pluripotency induction. Moreover, disruption of WWP2-mediated OCT4 ubiquitination during somatic cell reprogramming elevates OCT4 protein stability and *Ash2l-b* expression level, leading to higher H3K4 methylation levels and iPSC derivation efficiency. Therefore, this study highlights the important contribution of the post-translational modification on a key reprogramming factor to somatic cell reprogramming and exemplifies how a transcription factor coordinates with an epigenetic regulator to promote the cell fate conversion from somatic cells into PSCs.

RESULTS

Identification of Five Lysine Residues of OCT4 as Ub Conjugation Sites

We previously showed that WWP2 could catalyze OCT4 ubiquitination both *in vitro* and *in vivo*. However, the Ub acceptor sites of OCT4 remained unknown. We used a mutated form of Ub (K0), whose seven lysine residues were all replaced with arginine (R), in the *in vitro* ubiquitination reactions, to obtain specific and clear signals of ubiquitinated OCT4 (Table S1). Moreover, given that GST-WWP2 could ubiquitinate itself in the reaction interfering with the identification of ubiquitinated OCT4 by mass spectrometry (MS) analysis, His-OCT4 proteins were immunoprecipitated from the reaction product by high-affinity OCT4 antibodies (N124). The precipitated proteins were subsequently separated by gel electrophoresis, followed by Coomassie blue staining. Specific bands were sliced for MS analysis (Figure 1A). As a result, five lysine (K) residues (K118, K121, K133, K137, and K144) of OCT4 were identified as Ub conjugation sites (Figures 1B, top chart and S1). OCT4 consists of an N-transactivation domain, a POU domain, and a C-transactivation domain. The POU domain contains two structurally independent DNA binding domains (an NH2-terminal POU_S domain and a C-terminal POU_H domain). The five lysine residues locate across the N-terminal and POUs domains (Figure 1B, bottom panel).

To verify that the Ub acceptor sites identified by MS analysis, we displaced all these five Ks with R to generate an OCT4-5R mutant. In addition, the K118 residue of OCT4 was known to be also sumoylated (Zhang et al., 2007). To exclude the effect of sumoylation, we generated another OCT4 mutation construct (OCT4-4R), in which K121, K133, K137, and K144 were replaced by R, whereas K118 remained unchanged. To examine the potential function of each individual lysine residue, constructs for mutation of each single lysine residue were also generated. We performed *in vitro* ubiquitination reactions with both wild-type OCT4 (OCT4-WT) and mutated forms of OCT4 (OCT4-5R and OCT4-4R), as well as western blot analysis of the reaction products using Ub antibodies. In the presence of OCT4-WT, WWP2, Ub, as well as E1 and E2, strong signals at higher molecular weights indicative of Ub-modified OCT4-WT were detected (Figure 1C, lane 4). Notably, the ubiquitination signals for OCT4-5R and OCT4-4R were severely reduced compared with OCT4-WT (Figure 1C, lane 4 versus lanes 5 and 6), providing evidence that the five K residues should be the critical Ub conjugation sites of OCT4. Weak signals that remained with OCT4-5R and -4R could be caused by either nonspecific Ub modification after the specific sites were mutated, or unidentified Ub binding site(s) (Figure 1C, lanes 5 and 6). Meanwhile, auto-ubiquitinated WWP2 could be observed (Figure 1C, lane 3), showing the E3 ligase activity of WWP2 in these assays. Next, we tested whether one of the five Ks would be more important than others for OCT4 Ub modification using OCT4 constructs, each of which contained one K mutation to R. Our results that single K mutations only reduced

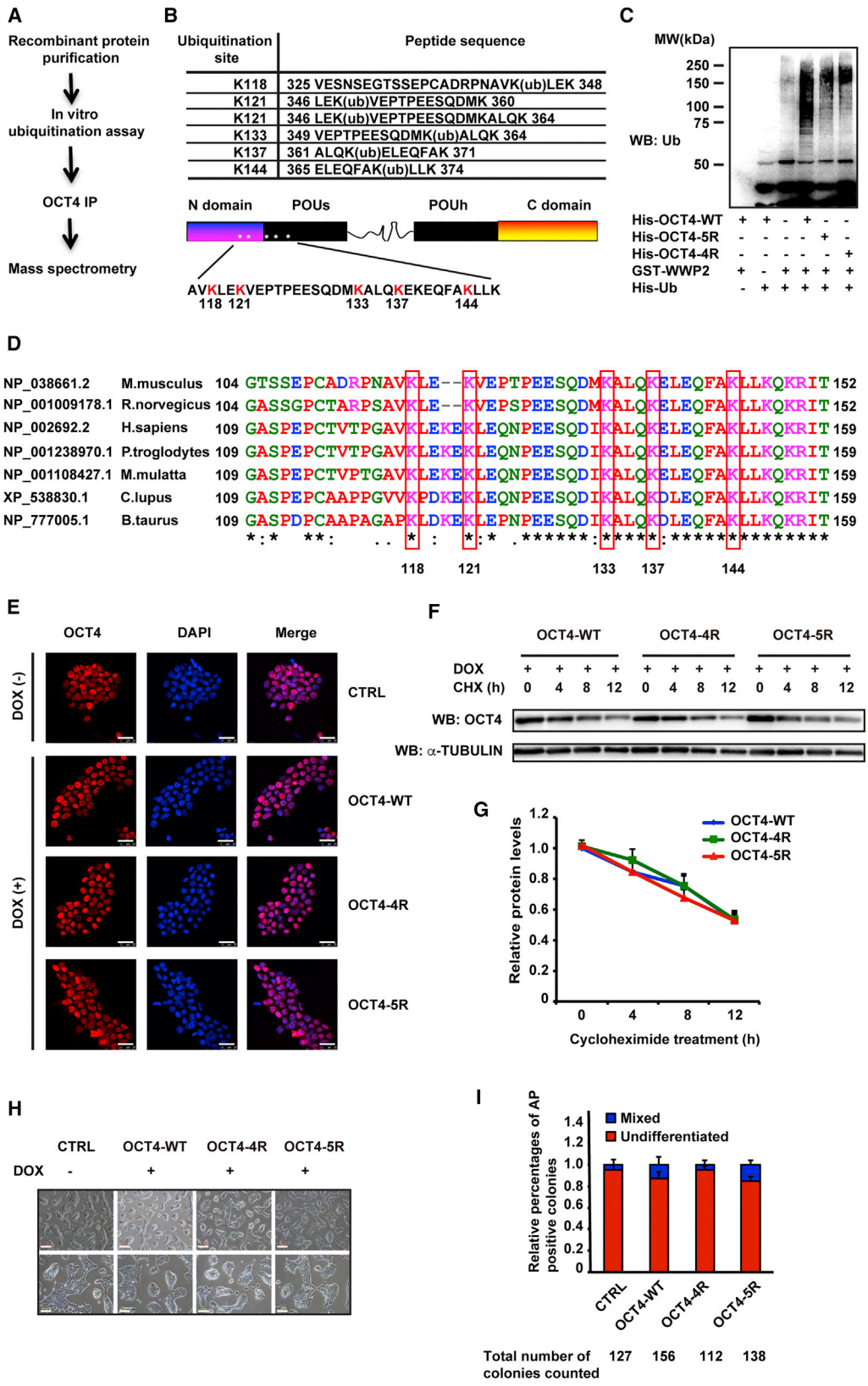

(legend on next page)

the level of ubiquitinated OCT4 slightly (Figures S2A and S2B), indicated that these five Ks together accounted for the major Ub accepting sites of OCT4. Of note, alignment of multiple OCT4 sequences revealed the full conservation of K118, K121, K133, K137, and K144 across a variety of mammalian species (Figure 1D), arguing that these sites are evolutionarily conserved to modulate OCT4 levels.

The identification of these five residues as Ub accepting sites of OCT4 enabled us to investigate the role of ubiquitination in the control of OCT4 functions. To test whether Ub modifications at these sites would affect OCT4 protein stability in undifferentiated ESCs, we overexpressed *Oct4-WT*, *-4R*, or *-5R* in mouse ESCs of line ZHBTc4, in which the endogenous *Oct4* was deleted and genetically integrated transgenic *Oct4* expression could be silenced by doxycycline (DOX) treatment (Niwa et al., 2000). This line provides an ideal system to study the function of ectopic *Oct4* in ESCs. We found that exogenous OCT4-WT, OCT4-5R, and OCT4-4R had similar expression levels and nuclear distribution, as validated by immunofluorescence (Figure 1E), and that they had comparable extents of OCT4 degradation and half-lives within a 12-hr period of treatment with cycloheximide (CHX) to block protein synthesis (Figures 1F and 1G). Thus, disruption of Ub modifications on these sites did not alter OCT4 protein stability. In addition, the half-life between transgenic OCT4 (in the absence of DOX) and OCT4-WT (in the presence of DOX) was similar, showing that the DOX treatment had no influence on the protein stability of OCT4 (Figure S3). Consistently, ESCs expressing *Oct4-4R* or *-5R* exhibited a typical doom-like shape of undifferentiated mouse ESC colonies, identical to ESCs expressing *Oct4-WT* (Figure 1H). To determine whether the self-renewal ability would be affected by these mutations, we performed colony formation assays and stained cells for the activity of alkaline phosphatase (AP), a method widely used for the evaluation of self-renewal capacity of PSCs (Figure 1I). As expected, high percentages of AP-positive colonies were found in all groups of cells tested, including ESCs treated with DOX expressing *Oct4-WT*, *-4R*, or *-5R* and ESCs without DOX treatment expressing the integrated transgenic *Oct4*.

Three out of five identified Ub modification sites located in the POUs domain, therefore we asked whether mutations of these lysine residues would affect DNA binding activities of OCT4. To address this issue, electrophoretic mobility gel shift assays were conducted with a PORE oligo probe (containing the consensus OCT4 binding sequence recognized by the POUs domain) (Esch et al., 2013) and purified recombinant proteins of OCT4 including WT, 5R, 4R, and single lysine residue mutants. OCT4-containing DNA-protein complexes were detected by the appearance of a shifted band. All the mutants had DNA binding capabilities similar to OCT4-WT (Figure S4A). Furthermore, the PORE probe could pull down the various OCT4 proteins

Figure 1. Identification of Five Lysine Residues of OCT4 as Its Ubiquitin Conjugation Sites

(A) Schematic illustration of the experimental design for *in vitro* OCT4 ubiquitination, immunoprecipitation (IP), and mass spectrometry (MS) analysis.

(B) Identification of K118, K121, K133, K137, and K144 as ubiquitinated residues at the N terminus of OCT4 by MS analysis. See also Figure S1.

(C) Mutations of five lysine residues abrogate WWP2-catalyzed ubiquitination of OCT4. Western blot analysis of ubiquitinated OCT4 protein levels using Ub antibodies after *in vitro* ubiquitination reactions. OCT4-5R carries the mutations of five lysine residues substituted by arginine (R) residues, and OCT4-4R carries the same lysine residue mutations as OCT4-5R, except for 118 lysine residues unchanged. Similar results were obtained from at least three independent experiments.

(D) Amino acid sequence alignment of the N-terminal domain of OCT4 orthologs from the mouse, rat, human, chimpanzee, monkey, wolf, and cattle (from top to bottom). Asterisks indicate full amino acid conservation and colons indicate partial conservation. Ubiquitinated lysine residues identified in the mouse OCT4 by MS analysis are boxed.

(E) Immunofluorescence staining of OCT4 using OCT4 antibodies (N124) in control ZHBTc4 ESCs (CTRL, without DOX) or ZHBTc4 ESCs (with doxycycline [DOX]) stably expressing *Oct4-WT*, *Oct4-4R*, or *Oct4-5R*. DAPI was used as a nuclear marker. Endogenous *Oct4* had been deleted and transgenic *Oct4* was silenced by DOX treatment in ZHBTc4 ESCs. Scale bars represent 25 μm. Similar results were obtained from at least three independent experiments.

(F) Mutations of ubiquitination residues have no effect on the protein stability of OCT4 in undifferentiated ESCs. Cycloheximide (CHX) was used to block protein synthesis and DOX was used for silencing transgenic *Oct4* expression. Western blotting was conducted with OCT4 antibodies (N124) to compare the protein levels among exogenous OCT4-WT, -4R, and -5R. α-TUBULIN was used as a loading control. See also Figure S3A.

(G) Protein half-life curves were made based on the data from (F). Error bars denote the means ± SD of three independent experiments. See also Figure S3B.

(H) Representative bright-field images of ZHBTc4 ESCs, and stable cell lines expressing *Oct4-WT*, *-4R*, and *-5R* with DOX addition. Scale bars represent 100 μm (upper panel) and 50 μm (lower panel). CTRL, control. Similar results were obtained from at least three independent experiments.

(I) Like OCT4-WT, OCT4-5R, and OCT4-4R can sustain ESC self-renewal. Mixed and undifferentiated colonies were counted after AP staining assays were conducted. Error bars denote the means ± SD of three independent experiments. AP, alkaline phosphatase.

overexpressed in HEK293 cells (Figure S4B). These results suggest that the mutations generated in our study do not disturb the DNA binding activity of OCT4, which might be a possible explanation to the fact that OCT4-5R and -4R could replace OCT4-WT functionally in ESCs.

In addition, we found that ESCs derived from *Wwp2* knockout (KO) mice (Yang et al., 2013) had a typical ESC morphology and expressed normal protein levels of pluripotent factors (OCT4, SOX2, and KLF4) (Figure S5). Collectively, these results indicate that WWP2 and WWP2-catalyzed OCT4 ubiquitination at these sites are dispensable for the maintenance of OCT4 protein stability and ESC self-renewal capacity when ESCs are at an undifferentiated state.

Mutation of the Five Lysine Residues Increases OCT4 Reprogramming Activity

As WWP2 regulates OCT4 protein levels in differentiating PSCs (Liao and Jin, 2010), we determined whether WWP2-catalyzed OCT4 ubiquitination would influence somatic cell reprogramming. MEFs were infected with retroviruses carrying full-length coding sequences of *Oct4(O)-WT* or *Oct4(O)-5R*, along with *Sox2(S)* and *Klf4(K)*. At 2 weeks post-infection, several ES-like cell colonies were picked up and cultured in the ESC medium. Both O(WT)SK and O(5R)SK could generate iPSCs. To characterize these iPSCs, we selected two iPSC lines for each *Oct4* type to assess the expression of ectopic *OSK* and endogenous *OSN* (*Nanog*). RT-PCR analysis showed that silencing of exogenous genes and activation of endogenous genes took place at passage 5 (Figure 2A). Of note, weak expression of ectopic *Oct4* and *Klf4* could still be detected in O(WT)SK-induced iPSCs, suggesting that the cells were not fully reprogrammed yet. We then verified the pluripotency potential of iPSCs by teratoma formation and germline transmission assays. In addition to the characteristic features of iPSC lines, we found that both O(5R)SK- and O(WT)SK-induced iPSCs gave rise to teratomas with 100% efficiency, and are chimera- and germ line-competent at passage 10 (Figures 2B and 2C).

During the process of iPSC line derivation, we noticed that more iPSC colonies formed in the O(5R)SK group than in the O(WT)SK group, suggesting that OCT4-5R might induce pluripotency more efficiently than OCT4-WT. To test this assumption, we compared reprogramming efficiencies of OCT4-WT, OCT4-4R, and OCT4-5R with MEFs prepared from the OG2 mice, which contained a transgenic *Oct4* regulatory sequence-driven *EGFP* reporter (Szabo et al., 2002) (Figure 3A). As a result, the efficiency of generating EGFP-positive iPSC colonies in MEFs expressing *Oct4-5R* was about ten times higher than that of MEFs expressing *Oct4-WT*, while a 3-fold increase was found in MEFs expressing *Oct4-4R* (Figure 3B). The finding indicated that disruption of WWP2-mediated OCT4 ubiquitination could promote the reprogramming process. As the reprogramming efficiency in MEFs expressing *Oct4-5R* was higher than that in MEFs expressing *Oct4-4R* (Figure 3B, column 2 versus column 3) and that the K118 residue could be modified by either Ub or a small ubiquitin-like modifier, we suspected that K118 sumoylation might influence reprogramming. To clarify this issue, we compared the reprogramming efficiency between MEFs expressing *Oct4-WT* and those expressing *Oct4-K118R* or *Oct4-E120A*. The two mutations were previously shown to abrogate OCT4 sumoylation (Zhang et al., 2007). We found similar numbers of EGFP-positive colonies in the three groups tested (Figure 3C), indicating that the disturbance of WWP2-mediated ubiquitination, rather than sumoylation, enhanced somatic cell reprogramming. Moreover, we found that *Wwp2* KO dramatically enhanced the reprogramming efficiency from MEFs (Figure 3D). Therefore, WWP2 and WWP2-mediated OCT4 Ub modification could serve as a barrier for successful somatic cell reprogramming. However, results from MEF reprogramming experiments using single lysine residue mutants of *Oct4* showed that none of the single lysine mutants interfered with the reprogramming efficiency (Figure 3E).

To characterize OCT4-5R-promoted pluripotency induction at a global scale, we conducted microarray analyses for cells collected at reprogramming days 3, 5, and 7 of both *Oct4-WT*- and *Oct4-5R*-expressing cells. Principal-component analysis illustrated that the transcriptional state of MEFs expressing *Oct4-5R* became ESC-like faster than MEFs expressing *Oct4-WT* (Figure 3F). In line with this result, the expression of up- and downregulated genes displayed faster change in cells expressing *Oct4-5R* than in those expressing *Oct4-WT* during the reprogramming process (Figure 3G). Thus, reprogramming using Ub modification-deficient OCT4 would enhance both efficiency and speed.

Deficiency in OCT4 Ubiquitination Enhances OCT4 Protein Stability and H3K4 Methylation Levels during Reprogramming Process

As WWP2-mediated OCT4 ubiquitination could promote OCT4 degradation through 26S proteasomes during differentiation of PSCs and in HEK293 cells (Liao and Jin, 2010; Xu et al., 2004), and that OCT4 levels have important impacts on somatic cell reprogramming (Papapetrou et al., 2009), we wanted to know whether the disruption of OCT4 ubiquitination would alter OCT4 protein levels during reprogramming. To answer the question, we examined dynamic changes in the steady-state levels of OCT4-WT, -4R, and -5R during MEF reprogramming. Western blot analysis showed that the protein levels of OCT4-WT, -4R, and -5R were comparable at reprogramming

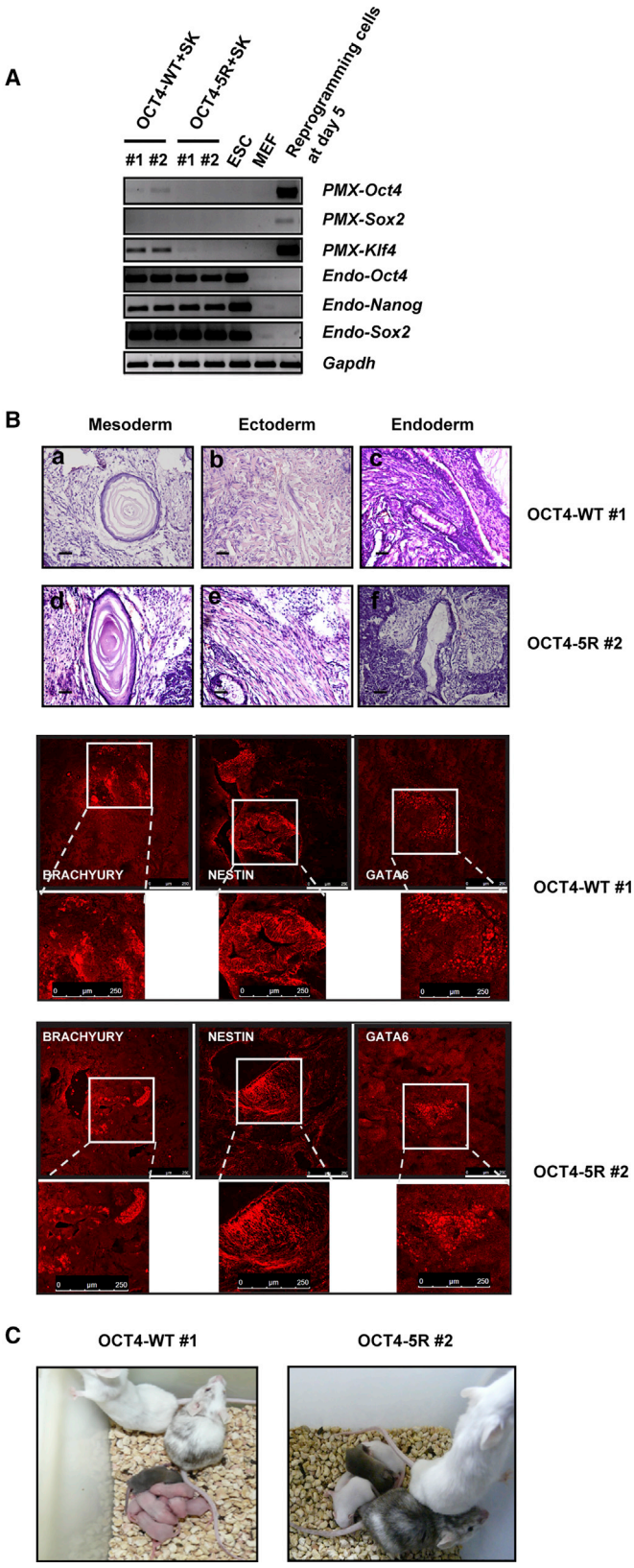

Figure 2. Characterization of iPSCs Induced from MEFs by OCT4-WT and OCT4-5R in Combination with SOX2 and KLF4

(A) RT-PCR analysis for transcript levels of reprogramming factors in cells as indicated. *Gapdh* was used as an internal control. PMX and Endo indicate exogenously and endogenously expressed factors, respectively. Similar results were obtained from at least three independent experiments. See also Table S2.

(B) H&E staining and immunofluorescence analysis of teratoma sections. Teratomas were formed by injection of OCT4-WT no. 1 iPSCs and OCT4-5R no. 2 iPSCs into the non-obese diabetic severe combined immunodeficiency mice, respectively. The antibodies against NESTIN, BRACHYUARY, and GATA6 were utilized to recognize ectoderm, mesoderm and endoderm, respectively. Scale bars represent 50 μm (H&E staining) and 250 μm (immunofluorescence).

(C) Germline transmission is successfully made from chimeric mice generated by blastocyst injection of OCT4-WT no. 1 and OCT4-5R no. 2 iPSCs, respectively.

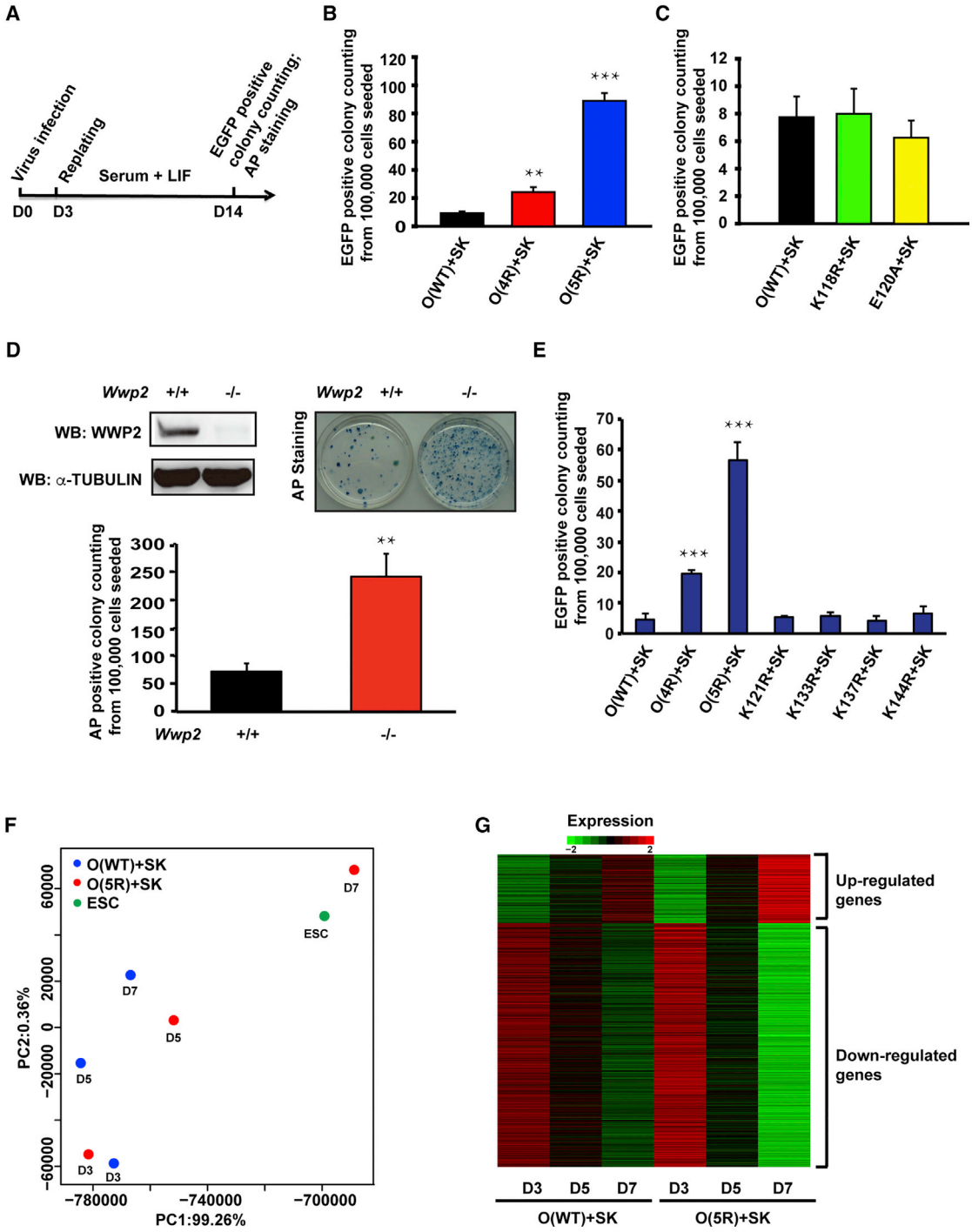

Figure 3. Disruption of WWP2-Mediated OCT4 Ubiquitination Enhances Reprogramming Efficiency and Speed

(A) Schematic illustration of the reprogramming process from the OG2 MEFs by viral transduction of *Oct4* (WT or ubiquitination mutants), *Sox2*, and *Klf4*. OG2 MEFs contain an *Oct4* regulatory sequence-regulated *Egfp* reporter cassette.

(B) Mutations of OCT4 ubiquitination sites induce reprogramming more effectively. Histograms represent mean numbers of OCT4-EGFP-expressing colonies counted at day 14. Error bars denote the means ± SD of three independent experiments. $^{**}p < 0.01$, $^{***}p < 0.001$, as determined by the Student's t test. OSK, OCT4, SOX2, and KLF4.

(legend continued on next page)

day 4 (Figure 4A, lanes 1, 5, and 9). However, levels of OCT4-WT declined evidently afterward, whereas levels of OCT4-4R and OCT4-5R remained relatively steady from day 5 to 7, implying that the protein stability of OCT4-4R and OCT4-5R might be higher than OCT4-WT at the intermediate stage of reprogramming. To provide direct evidence for this idea, we measured the OCT4 protein turnover rate in MEFs at reprogramming day 5. Indeed, OCT4-WT protein levels decreased substantially at 4 hr of CHX treatment, and could barely be detected at 8 and 12 hr. In contrast, proteins of OCT4-4R and OCT4-5R could be readily detected even at 12 hr after CHX treatment, albeit having lower levels than those at 0 hr (Figure 4B). The protein half-life curve showed that the protein stability of OCT4-5R and OCT4-4R was higher than that of OCT4-WT, but being comparable between the two mutants (Figure 4C). MG132, an inhibitor of 26S proteasome, enhanced the steady-state levels of proteins for both WT and mutant OCT4 at reprogramming day 5 (Figure S6A). The finding supported notions that OCT4 proteins are degraded through the 26 proteasomes (Liao and Jin, 2010) and that multiple E3 ligases target OCT4 for ubiquitination and degradation (Liao et al., 2013; Xu et al., 2004). Consistently, overexpression of *Wwp2* reduced the protein levels of OCT4-WT and single lysine mutants of OCT4 in HEK293 cells in a dose-dependent manner, which was blocked by MG132 treatment. Of note, WWP2 failed to promote protein degradation for OCT4-4R and OCT4-5R regardless of the presence or absence of MG132 (Figure S6B). These data further validate the key role of these five lysine residues for WWP2-mediated OCT4 protein degradation.

OCT4-5R induced MEF reprogramming with an obviously higher efficiency than OCT4-4R, although the two mutants degraded at a similar rate. This suggested that higher OCT4 protein levels could not fully account for higher reprogramming efficiency induced by OCT4 mutants. To find additional mechanisms, we examined levels of various histone methylations in MEFs at reprogramming days 5 and 8, looking for changes unique in the OCT4-5R group, since distinct histone methylation states are known to associate with the reprogramming process (Koche et al., 2011; Wang et al., 2017). Among all histone methylations tested, we consistently found higher levels of H3K4me1/2/3 in the OCT4-5R group compared with those in OCT4-WT and OCT4-4R groups (Figure 4D). It is likely that higher levels of H3K4 methylation observed in the OCT4-5R group gave rise to higher reprogramming efficiency, as several components of H3K4 methyltransferase complexes have been shown to be required for somatic cell reprogramming (Ang et al., 2011; Yang et al., 2015).

ASH2L-B Promotes Pluripotency Induction from Somatic Cells

To identify chromatin-modifying factors responsible for the higher H3K4 methylation level in the OCT4-5R group, we analyzed mRNA levels of H3K4 methyltransferase complex subunits of reprogramming MEFs at day 5 (Figure 4E) and found a higher level of *Ash2l-b* transcripts specifically in the OCT4-5R group compared with that in the OCT4-WT and OCT4-4R groups. There were no detectable variations in levels of the other subunits. In line with this finding, luciferase reporter assay results showed that OCT4-5R could activate the *Ash2l-b* promoter-driven reporter by about 13-fold compared with control, but did not impact the activity of *Ash2l-a* promoter-driven reporter (Figure S7), suggesting a specific effect of OCT4-5R in regulation *Ash2l-b* expression. These prompted us to further investigate the role of ASH2L-B in OCT4-5R-promoted somatic reprogramming.

(C) Sumoylation of OCT4 at K118 residue is dispensable for pluripotency induction. Histograms show reprogramming efficiencies from OG2 MEFs transduced with *Oct4-WT*, *Oct4-K118R*, or *Oct4-E120A* in combination with *Sox2* and *Klf4*. Error bars denote the means ± SD of three independent experiments.

(D) *Wwp2* knockout ($Wwp2^{-/-}$) promotes pluripotency induction. A representative image of AP staining of reprogrammed cells at day 14 (upper panel). Statistical analysis of numbers of AP-positive colonies from three independent experiments is shown to compare the difference in reprogramming efficiencies in the presence or absence of *Wwp2* (lower panel). MEFs from $Wwp2^{-/-}$ and wild-type ($Wwp2^{+/+}$) mice were reprogrammed by viral transduction of O(WT)SK reprogramming factors. Western blotting was conducted to validate the absence of WWP2 in $Wwp2^{-/-}$ MEFs. Error bars denote the means ± SD of three independent experiments. $^{**}p < 0.01$, as determined by the Student's t test.

(E) Single lysine residue mutation at K121, K133, K137, or K144 does not interfere with the efficiency of pluripotency induction from MEFs. The histogram shows reprogramming efficiencies of pluripotency induction from the OG2 MEFs, indicated by EGFP-positive colony numbers at reprogramming day 14. The reprogramming was induced by *Oct4-WT*, *Oct4-4R*, *Oct4-5R*, *Oct4-K121R*, *Oct4-K133R*, *Oct4-K137R*, or *Oct4-K144R*, respectively, in combination with *Sox2* and *Klf4*. Error bars denote the means ± SD of three independent experiments. $^{***}p < 0.001$, as determined by the Student's t test.

(F) OCT4-5R accelerates the reprogramming process. Principle component analysis of microarray data from ESCs and reprogramming MEFs overexpressing *O(WT)SK* or *O(5R)SK* at reprogramming days 3, 5, and 7.

(G) A heatmap shows changes in expression levels of up- and downregulated genes at reprogramming days 3, 5, and 7 in OCT4-WT and OCT4-5R groups.

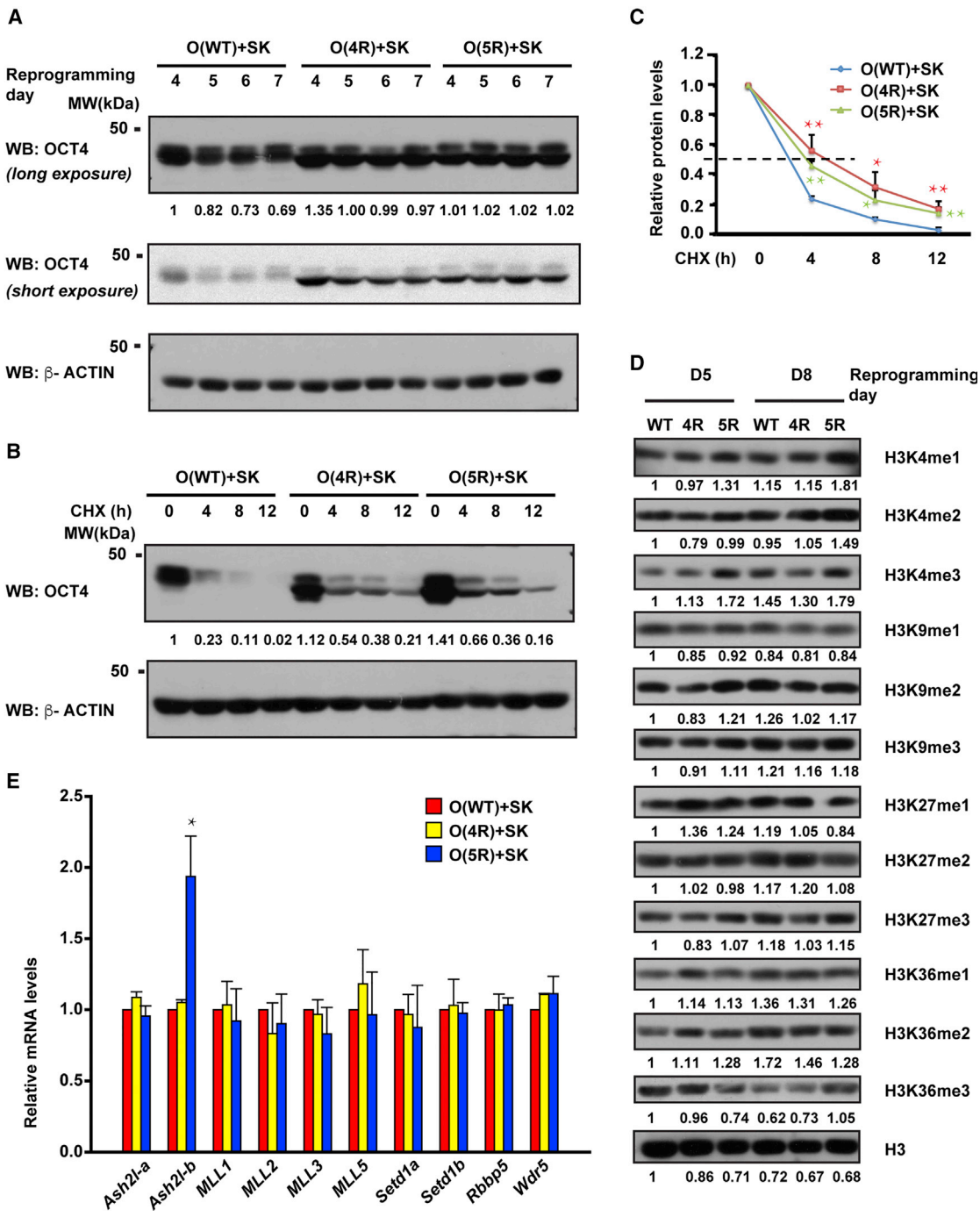

Figure 4. Mutations of OCT4 Ubiquitination Sites Increase OCT4 Protein Stability as Well as *Ash2l-b* Expression and H3K4 Methylation during Reprogramming Processes

(A) Examination of steady-state levels of OCT4-WT, -4R, and -5R proteins at reprogramming days 4, 5, 6, and 7 by western blotting. The level of β-ACTIN in each sample was used as a loading control. The similar results were obtained in at least three independent experiments.

(B) Levels of OCT4 proteins, including OCT4-WT, OCT4-4R, and OCT4-5R, were evaluated by western blotting using OCT4 antibodies. Samples were collected at reprogramming day 5, and cells were treated with CHX for different time lengths as indicated. The similar results were obtained in at least three independent experiments.

(C) Degradation rates of OCT4 proteins were analyzed based on the data from (B). Error bars denote the mean ± SD of three independent experiments. *$p < 0.05$, **$p < 0.01$, as determined by the Student's t test.

(legend continued on next page)

ASH2L has two prominent isoforms, ASH2L-A and ASH2L-B. They share the majority of the amino acid sequence and only vary at the N terminus (Figure 5A). It was reported that ASH2L is required for the maintenance of mouse ESCs at a self-renewal state (Wan et al., 2013). However, it was not clear which isoform contributes to the function. We found that ASH2L-B proteins were abundant in ESCs, but absent from adult cell types tested, whereas ASH2L-A proteins were broadly detected in various mouse tissues and organs in addition to in ESCs (Figure 5B). Moreover, *Ash2l-b* transcript levels declined drastically at day 3 and stayed at low levels in a spontaneous embryonic body differentiation model, while *Ash2l-a* levels fluctuated during the differentiation process (Figure 5C). The expression pattern of these two isoforms suggested a potential role of ASH2L-B in ESC maintenance. To determine whether ASH2L would be required for somatic cell reprogramming, we silenced *Ash2l* expression in OG2 MEFs using three sets of specific short hairpin RNA (shRNA) against *Ash2l*. Transfection of any one of the three *Ash2l* shRNAs blocked the generation of EGFP-positive iPSCs (Figure 5D), indicating the essential role of ASH2L for MEF reprogramming. However, the shRNAs used here could not distinguish the role of the two isoforms of *Ash2l*. To address this issue, we evaluated the OG2 MEF reprogramming efficiency in the presence of exogenous ASH2L-A or ASH2L-B along with O(WT)SK. Our result showed that overexpression of *Ash2-b* brought about an approximately 3-fold increase in reprogramming efficiency (Figure 5E). However, *Ash2l-a* overexpression had no impact on OSK-mediated MEF reprogramming. Together with the finding that *Ash2l-b*, but not *Ash2l-a*, was specifically induced by OCT4-5R during MEF reprogramming (Figure 4E), we propose that ASH2L-B is a positive regulator of somatic cell reprogramming and might contribute, at least partially, to the higher reprogramming efficiency and H3K4 methylation levels in OCT4-5R-promoted pluripotency induction.

OCT4 Binds and Regulates *Ash2l-b* Expression in ESCs

Given the specific expression pattern of ASH2L-B, we sought to explore how its expression was regulated. Using public datasets of transcription factor binding and epigenetic modification maps as well as the WASHU EPIGENOME BROWSER online tool, we analyzed features of *Ash2l* promoters, and found that H3K4me3 and H3K27ac, markers of active transcription, were enriched at the upstream regions next to the 5′ exons of both *Ash2l-a* and *-b*. However, POLR2A, a core component of the transcription machine, was markedly recruited to the promoter of *Ash2l-b*, but only weakly to the *Ash2l-a* promoter, in ESCs. Consistently, RNA sequencing results showed distinctive expression levels between the two isoforms in ESCs (Figure 6A, upper panel). Importantly, the promoter region of *Ash2l-b*, rather than *Ash2l-a*, was occupied by core transcription factors OCT4, SOX2, and NANOG in ESCs (Figure 6B). In contrast, MEFs had different epigenetic landscapes. H3K4me3, H3K27ac, and POLR2A vanished from the upstream region of *Ash2l-b*, while stronger binding of POLR2A occurred at the regulatory domain of *Ash2l-a* in MEFs compared with that in ESCs (Figure 6A, bottom panel). In line with this, *Ash2l-b* transcripts were not detected in MEFs. These data should pinpoint the distinct expression pattern and function between ASH2L-A and -B.

To obtain direct evidence that OCT4 could control *Ash2l-b* expression, we utilized mouse ESCs of the ZHBTc4 line (Niwa et al., 2000). DOX supplement led to the loss of *Oct4* expression rapidly in a few hours. Concomitantly, expression of *Ash2l-b*, but not *Ash2l-a*, declined gradually (Figure 6C), indicating that OCT4 could regulate *Ash2l-b* expression. In contrast, *Ash2l-a* expression elevated slightly upon DOX treatment, probably due to differentiation induced by silencing of *Oct4*. Moreover, our chromatin immunoprecipitation qPCR assays verified that OCT4 bound to the *Ash2l-b* promoter efficiently (Figures 6D and 6E). Collectively, these data suggest that the expression of the two isoforms of *Ash2l* are regulated differently under self-renewal and differentiating contexts, and OCT4, likely with other core transcription factors, directly governs the expression of *Ash2l-b* in ESCs.

DISCUSSION

OCT4 is a key factor of the transcriptional regulatory network governing not only establishment and maintenance of the pluripotent state but also exit from it. The array of studies demonstrates that OCT4 functions in a dosage-dependent manner: the absence of OCT4 in ESCs leads to the loss of self-renewal capability and differentiation toward the trophectoderm, whereas a 2-fold increase

(D) Levels of methylated histone 3 proteins in cells at reprogramming days 5 and 8 were compared among OCT4-WT, -4R, and -5R groups. A representative western blot result of three independent experiments is shown.
(E) A histogram represents the relative gene expression levels of members of the TrxG family at reprogramming day 5 determined by qRT-PCR assays. The mRNA level in MEFs expressing *Oct4-WT*, *Sox2*, and *Klf4* was set at as 1. Error bars denote the means ± SD of three independent experiments. *$p < 0.05$, as analyzed by Student's t test.
See also Table S2.

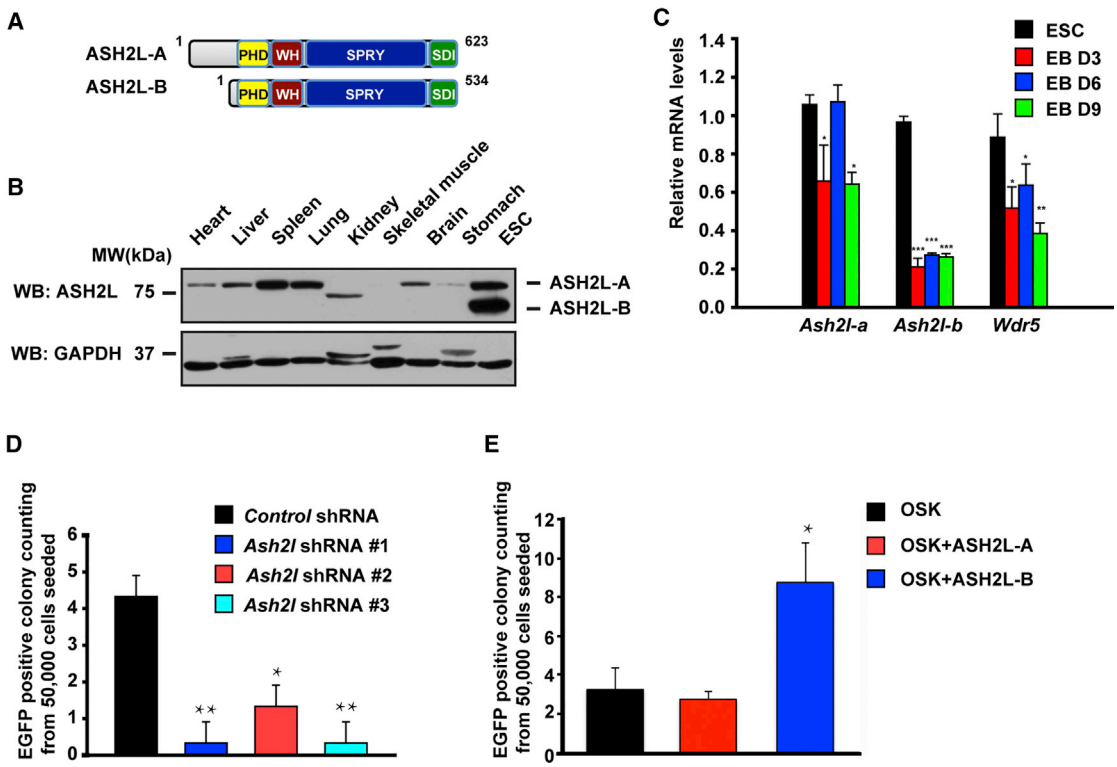

Figure 5. ASH2L-B Engages in the Induction of Pluripotency

(A) Schematic illustration of the protein domain for the two isoforms of ASH2L, ASH2L-A, and ASH2L-B, including the PHD region (yellow), WH region (dark red), SPRY region (blue), and SDI region (green).

(B) Western blot analysis of protein levels of ASH2L-A and ASH2L-B in ESCs and various issues/organs collected from adult mice. Anti-ASH2L antibodies recognize both ASH2L-A and ASH2L-B. GAPDH levels were used as a loading control. A representative western blot result of three independent experiments is shown.

(C) A histogram represents qRT-PCR results of *Ash2l-a*, *Ash2l-b*, and *Wdr5* transcript levels during embryoid body (EB) formation at the indicated time points (days 3, 6, and 9). Error bars denote the means ± SD of three independent experiments. *p < 0 .05, **p < 0.01, ***p < 0.001, as determined by Student's t test.

(D) A histogram shows OCT4-EGFP-positive colony numbers at reprogramming day 14. OG2 MEFs (50,000) were transduced with *Ash2l* shRNA (*Ash2l* shRNA nos 1–3) or control shRNA together with O(WT)SK reprogramming factors. Error bars denote the means ± SD of three independent experiments. *p < 0.05 and **p < 0.01, as analyzed by Student's t test.

(E) A histogram shows numbers of the OCT4-EGFP-positive colony from 50,000 MEFs expressing ASH2L-A or ASH2L-B in combination with OCT4, SOX2, and KLF4 (OSK). Error bars denote the means ± SD of three independent experiments. *p < 0.05, as analyzed by Student's t test.

in the OCT4 level induces differentiation into primitive endoderm and mesoderm (Niwa et al., 2000). Recently, Karwacki-Neisius et al. (2013) reported that reduced *Oct4* expression (*Oct4*$^{+/-}$) defines a robust pluripotent state and that a normal range of OCT4 allows effective differentiation. Moreover, Radzisheuskaya et al. (2013) proposed that a proper range of OCT4 protein levels governs cell state transitions, such as pluripotency entry and exit. However, OCT4 levels can be reduced down to 7-fold without loss of self-renewal once pluripotency is established. These studies underscore the significance of OCT4 protein levels in pluripotency entry, maintenance, and exit. However, how the amount of OCT4 proteins is precisely regulated, particularly at a post-translational level, is far from completely understood.

Herein, we reveal that disruption of OCT4 ubiquitination exerts favorable effects on the efficiency and speed of pluripotency induction, indicating that the elevation of OCT4 protein stability could expedite the reprogramming process. A previous study defined the optimal stoichiometry of reprogramming factors used for the induction of pluripotency and proposed a combination of an equal dosage of SOX2, KLF4, and c-MYC, with a 3-fold dosage of OCT4, as an efficient strategy (Papapetrou et al., 2009). Nevertheless, this optimized combination elicited only approximately 2-fold increase in the reprogramming

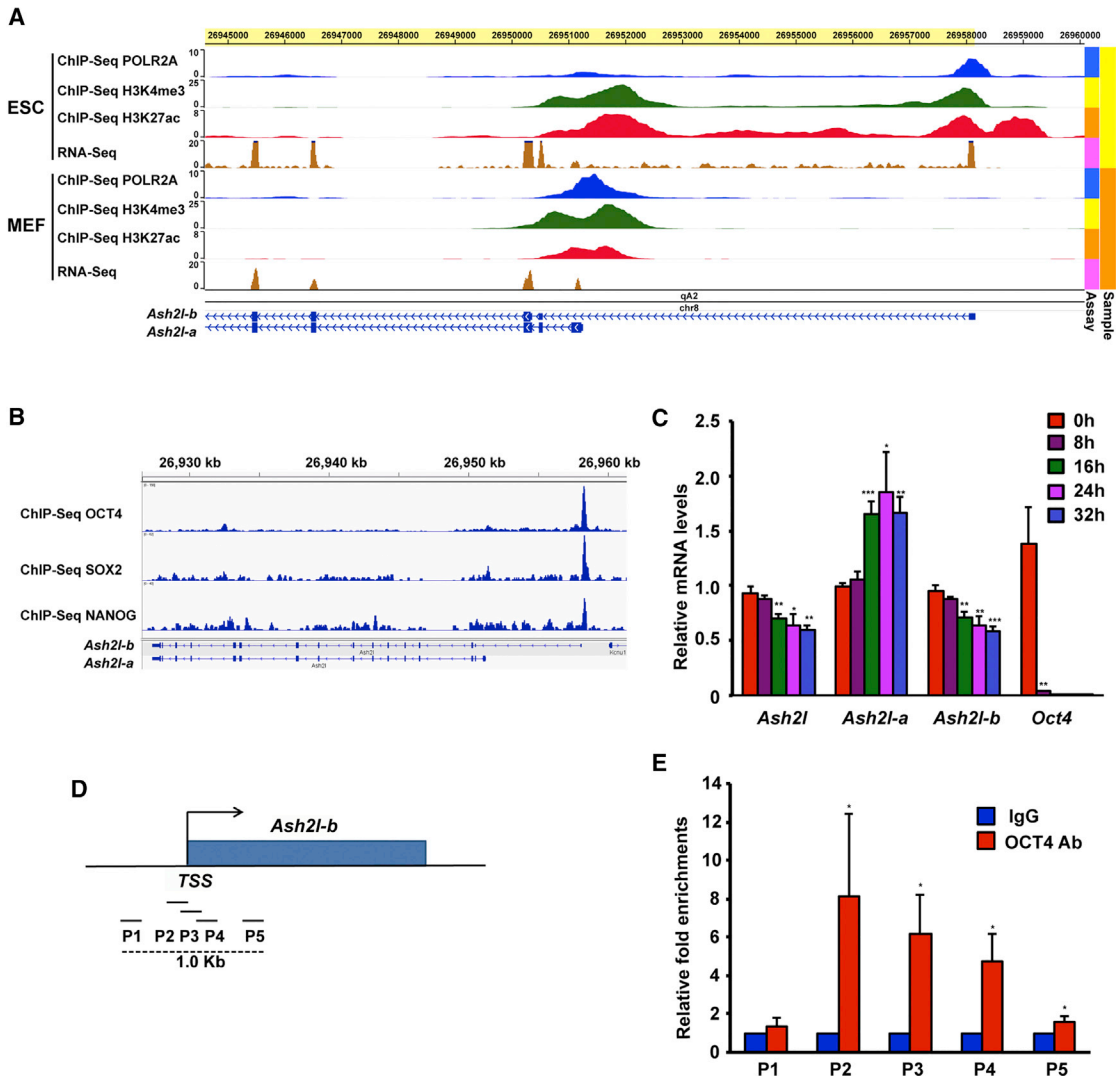

Figure 6. The Expression of *Ash2l-b* Is Regulated by OCT4 in ESCs

(A) Tracks of chromatin immunoprecipitation sequencing (ChIP-seq) and RNA sequencing (RNA-seq) showing enrichments of POLR2A, H3K4me3, and H3K27ac at genomic loci of *Ash2l-a* and *Ash2l-b*, as well as their expression levels in ESCs and MEFs.

(B) ChIP-seq tracks showing that the promoter region of *Ash2l-b*, rather than *Ash2l-a*, was occupied by OCT4, SOX2, and NANOG in ESCs.

(C) qRT-PCR analysis for mRNA levels of *Ash2l* (total), *Ash2l-a*, *Ash2l-b*, and *Oct4* during ZHBTc4 ESC differentiation induced by DOX treatment. Data are shown as means ± SD of three independent experiments. *$p < 0.05$, **$p < 0.01$, ***$p < 0.001$, as analyzed by the Student's t test.

(D) A schematic illustration for the location of amplicons utilized to evaluate the enrichment of OCT4 at the *Ash2l-b* promoter by ChIP-qPCR assays. TSS, transcription start site.

(E) Results of ChIP-qPCR assay using OCT4 antibodies in J1 ESCs. Relative fold enrichments are shown. The value from the control immunoglobulin G (IgG) ChIP-qPCR was set as 1. Data are presented as means ± SD of four independent experiments. *$p < 0.05$, as analyzed by Student's t test.

See also Table S3.

efficiency. In the current study, OCT4-5R could give rise to a 10-fold increase compared with OCT4-WT in a combination with SOX2 and KLF4. Therefore, this mutant OCT4 brings a significant advantage over OCT4-WT for pluripotency induction from somatic cells. Given that *Wwp2* KO MEFs also have higher reprogramming efficiency than WT MEFs, we surmise that WWP2-mediated OCT4 ubiquitination and degradation interferes with reprogramming. Our finding that disruption of WWP2-catalyzed OCT4 ubiquitination enhances the OCT4 protein stability and

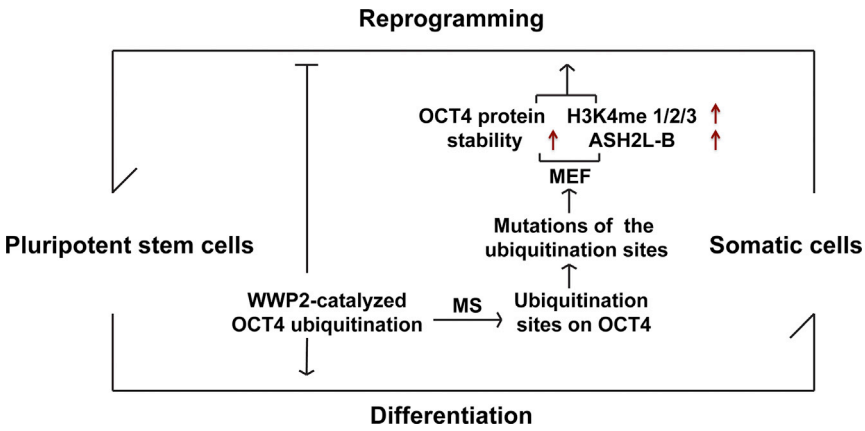

Figure 7. A Schematic Summary of this Study

Mass spectrometric analysis of WWP2-catalyzed ubiquitinated OCT4 proteins identifies five Ub conjugation lysine residues. Mutations of these Ub conjugation sites enhance the ability of OCT4 to induce pluripotency from MEFs significantly. The increase in the OCT4 protein stability, as well as expression of *Ash2l-b* and H3K4 methylation during somatic cell reprogramming, might contribute to the enhanced reprogramming efficiency observed with OCT4 mutants deficient in WWP2-mediated ubiquitination.

efficiency of pluripotency entry, opens a new avenue to optimize the iPSC technique.

Several years ago, Lu et al. (2012) reported that miR-25 could enhance the production of iPSCs induced by the four OSKM factors from MEF. Interestingly, they found that *Wwp2* was one of the targets of miR-25, having lower expression levels in iPSCs reprogrammed by miR-25 plus OSKM than in iPSCs reprogramming by the four factors alone. Consistently, we found that *Wwp2*-null MEFs could be induced by the O(WT)SK at higher efficiencies than WT cells. Nevertheless, we are not certain whether the enhanced reprogramming efficiency in *Wwp2*-null MEF would share molecular mechanisms by which OCT4-5R regulates reprogramming. WWP2 has other substrates in addition to OCT4 and participates in various biological processes (Maddika et al., 2011; Soond and Chantry, 2011; Yang et al., 2013; Yu et al., 2016). It is possible that alterations in levels of its other substrates would also contribute to enhanced pluripotency induction in *Wwp2*-null MEFs. On the other hand, our previous study identified ITCH as an E3 Ub ligase of OCT4 and ITCH controls OCT4 ubiquitination and transcriptional activity in undifferentiated ESCs (Liao et al., 2013). Therefore, similar to other key proteins, such as p53, OCT4 has more than one Ub ligases and these ligases function in a cell state-dependent manner.

Intriguingly, OCT4-4R promoted reprogramming less efficiently than OCT4-5R, although both mutations enhanced OCT4 protein stability to the similar extent. This suggests that, in addition to enhancing OCT4 protein stability, OCT4-5R has additional abilities that OCT4-4R does not share. Indeed, we uncovered that *Ash2l-b*, a gene encoding one of the core components of MLL H3K4 methyltransferase, is a direct target of OCT4, and that OCT4-5R activated its expression to a significantly higher level than OCT4-WT and OCT4-4R during MEF reprogramming. ASHL-B might promote reprogramming through elevating H3K4 methylation levels. In addition, we found that OCT4-5R activated *Ash2l-b* promoter-driven reporter activities by about 13-fold compared with control, but did not activate *Ash2l-a* promoter-driven reporter activities, suggesting a specific effect of OCT4-5R in regulation of *Ash2l-b* expression. In contrast, OCT4-WT activated *Ash2l-b* promoter-driven reporter activities by only about 2-fold. Therefore, we propose that enhanced OCT4 protein stability, as well as *Ash2l-b* expression and H3K4 methylation, might both contribute to OCT4-5R-promoted somatic reprogramming (Figure 7).

We currently do not know why OCT4-5R has a stronger ability to activate *Ash2l-b* expression than OCT4-WT and OCT4-4R. The mutation in OCT4-5R might alter the protein conformation favoring its interaction with other transcriptional co-activators or regulatory regions of OCT4 target genes. Further studies are needed to address the question. Nevertheless, the OCT4-ASH2L-H3K4me axis identified in this study sheds lights on the crosstalk between transcription factor and epigenetic control during somatic cell reprogramming.

EXPERIMENTAL PROCEDURES

Animals

All the animal experiments were approved by our institution and conducted under the Guideline for Animal Care at Shanghai Jiao Tong University School of Medicine.

Identification of Ubiquitination Sites of OCT4

In vitro ubiquitination reactions were set up as described in Table S1. In brief, rabbit E1 (50 ng, Merck), His-Ub-carrier enzyme H6 (0.4 μg, Merck), GST-WWP2 (0.4 μg), His-OCT4 (1 μg), and His-Ub-K0 or -WT (2 μg, Merck) were added to the ubiquitination buffer (50 mM Tris-HCl [pH 7.4], 2 mM ATP, 5 mM $MgCl_2$, and 2 mM dithiothreitol) to a final volume of 30 μL. After incubation at 30°C for 2 hr, the reaction mixtures were denatured with

1% SDS and 5% β-mercaptoethanol supplement at 100°C for 10 min, followed by dilution of the volume by 10-fold with 1× PBS buffer. His-tagged OCT4 proteins from *in vitro* ubiquitination reactions were pulled down utilizing specific antibodies against OCT4 (N124), resolved in an 8% SDS-PAGE gel, and visualized by Coomassie blue staining. The protein in-gel digestion and peptide identification by nano-high-pressure liquid chromatography-MS were conducted as described previously (Xu et al., 2004).

Preparation of GST or His Fusion Proteins and *In Vitro* Ubiquitination Assays

GST and His fusion proteins were expressed and purified according to the manufacturer's instructions (from Amersham Biosciences and Novagen, respectively). *In vitro* ubiquitination assays were conducted as described previously (Liao and Jin, 2010).

Viral Preparation and iPSC Line Derivation

Viral preparation and iPSC line derivation were conducted as described previously (Liao et al., 2013). In brief, retroviral *Oct4* (WT and mutants), *Sox2*, *Klf4*, *Ash2l-a*, and *Ash2l-b* were produced in Plat-E cells, and lentiviral *shAsh2l* packaging was performed in 293FT cells. To generate iPSCs, 1×10^5 OG2 MEFs were infected with viral supernatants. Fourteen days later, OCT4-EGFP-positive colonies were scored and picked up for iPSC line establishment. Detailed procedures are provided in Supplemental Experimental Procedures.

Protein Stability Assays with CHX

Cells were cultured with CHX (Sigma-Aldrich) at a concentration of 50 μg/mL for the indicated times. Then, cells were collected and subjected to western blotting to visualize protein levels.

Statistical Analysis

Values are presented as means ± SD. Comparisons between two different groups were determined utilizing the Student's t test. Differences with a p value <0.05 were considered statistically significant.

ACCESSION NUMBERS

The microarray data from this publication have been submitted to the GEO database under the accession number GEO: GSE111397.

SUPPLEMENTAL INFORMATION

Supplemental Information includes Supplemental Experimental Procedures, seven figures, and three tables and can be found with this article online at https://doi.org/10.1016/j.stemcr.2018.09.001.

AUTHOR CONTRIBUTIONS

B.L. and Y.J. developed the project, interpreted the data, and wrote the manuscript. S.L. and F.X. performed most of experiments and data analysis. X.S. and H.W. contributed to ESC culture. Y. Zeng contributed to microarray data analyses. J.H. contributed to plasmid constructions. F.T. contributed to teratoma section and histological analyses. J.G. contributed to teratoma assays and MEF derivation. J.Z. and Y. Zhao contributed to mass spectrometry analyses.

ACKNOWLEDGMENTS

We would like to thank Jinsong Li from the Institute of Biochemistry and Cell Biology, CAS, for providing TgOG2 *Oct4*-EGFP transgenic mice; Austin Smith from the University of Cambridge for providing CGR8 ESC lines; and Xiaohua Shen from Tsinghua University for providing J1 ESC lines. This work was supported by grants from the Ministry of Science and Technology of China (2016YFA0100100), the National Natural Science Foundation of China (31471231, 31730055, and 31471393), the Shanghai Pujiang Program (16PJD031), and the Strategic Priority Research Program of the Chinese Academy of Sciences (XDB19020100 and XDA01010102).

Received: March 16, 2018
Revised: September 3, 2018
Accepted: September 3, 2018
Published: September 27, 2018

REFERENCES

Ang, Y.S., Tsai, S.Y., Lee, D.F., Monk, J., Su, J., Ratnakumar, K., Ding, J., Ge, Y., Darr, H., Chang, B., et al. (2011). Wdr5 mediates self-renewal and reprogramming via the embryonic stem cell core transcriptional network. Cell *145*, 183–197.

Buckley, S.M., Aranda-Orgilles, B., Strikoudis, A., Apostolou, E., Loizou, E., Moran-Crusio, K., Farnsworth, C.L., Koller, A.A., Dasgupta, R., Silva, J.C., et al. (2012). Regulation of pluripotency and cellular reprogramming by the ubiquitin-proteasome system. Cell Stem Cell *11*, 783–798.

Dou, Y., and Hess, J.L. (2008). Mechanisms of transcriptional regulation by MLL and its disruption in acute leukemia. Int. J. Hematol. *87*, 10–18.

Dou, Y., Milne, T.A., Ruthenburg, A.J., Lee, S., Lee, J.W., Verdine, G.L., Allis, C.D., and Roeder, R.G. (2006). Regulation of MLL1 H3K4 methyltransferase activity by its core components. Nat. Struct. Mol. Biol. *13*, 713–719.

Esch, D., Vahokoski, J., Groves, M.R., Pogenberg, V., Cojocaru, V., Vom Bruch, H., Han, D., Drexler, H.C., Arauzo-Bravo, M.J., Ng, C.K., et al. (2013). A unique Oct4 interface is crucial for reprogramming to pluripotency. Nat. Cell Biol. *15*, 295–301.

Evans, M.J., and Kaufman, M.H. (1981). Establishment in culture of pluripotential cells from mouse embryos. Nature *292*, 154–156.

Jang, H., Kim, T.W., Yoon, S., Choi, S.Y., Kang, T.W., Kim, S.Y., Kwon, Y.W., Cho, E.J., and Youn, H.D. (2012). O-GlcNAc regulates pluripotency and reprogramming by directly acting on core components of the pluripotency network. Cell Stem Cell *11*, 62–74.

Karwacki-Neisius, V., Goke, J., Osorno, R., Halbritter, F., Ng, J.H., Weisse, A.Y., Wong, F.C., Gagliardi, A., Mullin, N.P., Festuccia, N., et al. (2013). Reduced Oct4 expression directs a robust pluripotent state with distinct signaling activity and increased enhancer occupancy by Oct4 and Nanog. Cell Stem Cell *12*, 531–545.

Kim, J.B., Greber, B., Arauzo-Bravo, M.J., Meyer, J., Park, K.I., Zaehres, H., and Scholer, H.R. (2009a). Direct reprogramming of human neural stem cells by OCT4. Nature *461*, 649–653.

Kim, J.B., Sebastiano, V., Wu, G., Arauzo-Bravo, M.J., Sasse, P., Gentile, L., Ko, K., Ruau, D., Ehrich, M., van den Boom, D., et al. (2009b). Oct4-induced pluripotency in adult neural stem cells. Cell *136*, 411–419.

Koche, R.P., Smith, Z.D., Adli, M., Gu, H., Ku, M., Gnirke, A., Bernstein, B.E., and Meissner, A. (2011). Reprogramming factor expression initiates widespread targeted chromatin remodeling. Cell Stem Cell *8*, 96–105.

Liao, B., and Jin, Y. (2010). Wwp2 mediates Oct4 ubiquitination and its own auto-ubiquitination in a dosage-dependent manner. Cell Res. *20*, 332–344.

Liao, B., Zhong, X., Xu, H., Xiao, F., Fang, Z., Gu, J., Chen, Y., Zhao, Y., and Jin, Y. (2013). Itch, an E3 ligase of Oct4, is required for embryonic stem cell self-renewal and pluripotency induction. J. Cell. Physiol. *228*, 1443–1451.

Liu, L., Michowski, W., Inuzuka, H., Shimizu, K., Nihira, N.T., Chick, J.M., Li, N., Geng, Y., Meng, A.Y., Ordureau, A., et al. (2017). G1 cyclins link proliferation, pluripotency and differentiation of embryonic stem cells. Nat. Cell Biol. *19*, 177–188.

Lu, D., Davis, M.P., Abreu-Goodger, C., Wang, W., Campos, L.S., Siede, J., Vigorito, E., Skarnes, W.C., Dunham, I., Enright, A.J., and Liu, P. (2012). MiR-25 regulates Wwp2 and Fbxw7 and promotes reprogramming of mouse fibroblast cells to iPSCs. PLoS One *7*, e40938.

Maddika, S., Kavela, S., Rani, N., Palicharla, V.R., Pokorny, J.L., Sarkaria, J.N., and Chen, J. (2011). WWP2 is an E3 ubiquitin ligase for PTEN. Nat. Cell Biol. *13*, 728–733.

Nichols, J., Zevnik, B., Anastassiadis, K., Niwa, H., Klewe-Nebenius, D., Chambers, I., Scholer, H., and Smith, A. (1998). Formation of pluripotent stem cells in the mammalian embryo depends on the POU transcription factor Oct4. Cell *95*, 379–391.

Niwa, H., Miyazaki, J., and Smith, A.G. (2000). Quantitative expression of Oct-3/4 defines differentiation, dedifferentiation or self-renewal of ES cells. Nat. Genet. *24*, 372–376.

Papapetrou, E.P., Tomishima, M.J., Chambers, S.M., Mica, Y., Reed, E., Menon, J., Tabar, V., Mo, Q., Studer, L., and Sadelain, M. (2009). Stoichiometric and temporal requirements of Oct4, Sox2, Klf4, and c-Myc expression for efficient human iPSC induction and differentiation. Proc. Natl. Acad. Sci. USA *106*, 12759–12764.

Radzisheuskaya, A., Chia Gle, B., dos Santos, R.L., Theunissen, T.W., Castro, L.F., Nichols, J., and Silva, J.C. (2013). A defined Oct4 level governs cell state transitions of pluripotency entry and differentiation into all embryonic lineages. Nat. Cell Biol. *15*, 579–590.

Ruthenburg, A.J., Allis, C.D., and Wysocka, J. (2007). Methylation of lysine 4 on histone H3: intricacy of writing and reading a single epigenetic mark. Mol. Cell *25*, 15–30.

Saxe, J.P., Tomilin, A., Scholer, H.R., Plath, K., and Huang, J. (2009). Post-translational regulation of Oct4 transcriptional activity. PLoS One *4*, e4467.

Soond, S.M., and Chantry, A. (2011). Selective targeting of activating and inhibitory Smads by distinct WWP2 ubiquitin ligase isoforms differentially modulates TGFbeta signalling and EMT. Oncogene *30*, 2451–2462.

Steward, M.M., Lee, J.S., O'Donovan, A., Wyatt, M., Bernstein, B.E., and Shilatifard, A. (2006). Molecular regulation of H3K4 trimethylation by ASH2L, a shared subunit of MLL complexes. Nat. Struct. Mol. Biol. *13*, 852–854.

Szabo, P.E., Hubner, K., Scholer, H., and Mann, J.R. (2002). Allele-specific expression of imprinted genes in mouse migratory primordial germ cells. Mech. Dev. *115*, 157–160.

Takahashi, K., Tanabe, K., Ohnuki, M., Narita, M., Ichisaka, T., Tomoda, K., and Yamanaka, S. (2007). Induction of pluripotent stem cells from adult human fibroblasts by defined factors. Cell *131*, 861–872.

Takahashi, K., and Yamanaka, S. (2006). Induction of pluripotent stem cells from mouse embryonic and adult fibroblast cultures by defined factors. Cell *126*, 663–676.

Thomson, J.A., Itskovitz-Eldor, J., Shapiro, S.S., Waknitz, M.A., Swiergiel, J.J., Marshall, V.S., and Jones, J.M. (1998). Embryonic stem cell lines derived from human blastocysts. Science *282*, 1145–1147.

Wan, M., Liang, J., Xiong, Y., Shi, F., Zhang, Y., Lu, W., He, Q., Yang, D., Chen, R., Liu, D., et al. (2013). The trithorax group protein Ash2l is essential for pluripotency and maintaining open chromatin in embryonic stem cells. J. Biol. Chem. *288*, 5039–5048.

Wang, Y., Bi, Y., and Gao, S. (2017). Epigenetic regulation of somatic cell reprogramming. Curr. Opin. Genet. Dev. *46*, 156–163.

Wei, F., Scholer, H.R., and Atchison, M.L. (2007). Sumoylation of Oct4 enhances its stability, DNA binding, and transactivation. J. Biol. Chem. *282*, 21551–21560.

Xu, H., Wang, W., Li, C., Yu, H., Yang, A., Wang, B., and Jin, Y. (2009). WWP2 promotes degradation of transcription factor OCT4 in human embryonic stem cells. Cell Res. *19*, 561–573.

Xu, H.M., Liao, B., Zhang, Q.J., Wang, B.B., Li, H., Zhong, X.M., Sheng, H.Z., Zhao, Y.X., Zhao, Y.M., and Jin, Y. (2004). Wwp2, an E3 ubiquitin ligase that targets transcription factor Oct-4 for ubiquitination. J. Biol. Chem. *279*, 23495–23503.

Yang, Y., Liao, B., Wang, S., Yan, B., Jin, Y., Shu, H.B., and Wang, Y.Y. (2013). E3 ligase WWP2 negatively regulates TLR3-mediated innate immune response by targeting TRIF for ubiquitination and degradation. Proc. Natl. Acad. Sci. USA *110*, 5115–5120.

Yang, Z., Augustin, J., Hu, J., and Jiang, H. (2015). Physical interactions and functional coordination between the core subunits of Set1/Mll complexes and the reprogramming factors. PLoS One *10*, e0145336.

Yu, Z., Li, T., Wang, C., Deng, S., Zhang, B., Huo, X., Zhang, B., Wang, X., Zhong, Y., and Ma, X. (2016). Gamabufotalin triggers c-Myc degradation via induction of WWP2 in multiple myeloma cells. Oncotarget *7*, 15725–15737.

Zhang, Z., Liao, B., Xu, M., and Jin, Y. (2007). Post-translational modification of POU domain transcription factor Oct-4 by SUMO-1. FASEB J. *21*, 3042–3051.